Reversible Dissociation and Conformational Stability of Dimeric Ribulose Bisphosphate Carboxylase†

Leonardo Erijman,‡ George H. Lorimer,§ and Gregorio Weber*,‡

Department of Biochemistry, University of Illinois, Urbana, Illinois 61801, and Molecular Biology Division, Central Research and Development, Du Pont Company, Experimental Station, Wilmington, Delaware 19880-0402

Received November 11, 1992; Revised Manuscript Received March 5, 1993

ABSTRACT: Dimer–monomer dissociation of ribulosebisphosphate carboxylase/oxygenase from *Rhodospirillum rubrum* was investigated using hydrostatic pressure in the range 1–2 kbar to promote dissociation. Intrinsic fluorescence emission and polarization, along with the polarization of the fluorescence of single-labeled AEDANS conjugates, were used to follow the dissociation. Full reversibility after dissociation was observed to depend on the presence of small ligands: glycerol, Mg^{2+}, and $NaHCO_3$, the last two being required to activate the enzyme. The free energy of association at 15 °C, −12.9 kcal mol^{-1}, was made up of a positive change in enthalpy on association of 6.0 kcal mol^{-1} and an entropic contribution ($T\Delta S$) of 18.9 kcal mol^{-1}; thus the monomer association is entropy driven. No dissociation of the quaternary complex formed by the dimer, 2-carboxy-D-arabinitol 1,5-diphosphate (CADP), Mg^{2+}, and $NaHCO_3$ was observed at pressures up to 2.0 kbar; the magnitude of stabilization by the inhibitor binding was estimated as 2.3 kcal mol^{-1}. Pressurization in the presence of bis-ANS results in a time-dependent increase in fluorophore emission, indicating changes in monomer conformation with exposure of hydrophobic surfaces upon dissociation. Reactivity against the fluorescent probe 1,5-I-AEDANS was also used as a conformational probe: HPLC of a trypsin digest of rubisco labeled at atmospheric pressure revealed a single fluorescent peptide, whereas more extensive labeling was observed when the reaction was carried out at 2.0 kbar, indicative of exposure of internal cysteines. Most of the properties of the monomeric species detected at high hydrostatic pressure, namely, the red-shifted tryptophan emission relative to the native dimer, binding of hydrophobic probes, and instability at high concentrations and at temperatures above 15 °C, suggest those of the previously described folding intermediate (van der Vies, S. M., Viitanen, P. V., Gatenby, A. A., Lorimer, G. H., & Jaenicke, R. (1992) *Biochemistry 31*, 3635–3644). Further information about intersubunit affinity was obtained by reexamination of the enzyme carrying a single mutation, K168E (Mural, R. J., Soper, T. S., Larimer, F. W., & Hartman, F. (1990) *J. Biol. Chem. 265*, 6501–6505), previously described as a "folded monomer". By using size-exclusion HPLC, dilution, and fluorescence polarization at high pressure, we demonstrate that although the mutant shows a decrease in dissociation constant of 2 orders of magnitude compared with the wild-type enzyme, it is still able to form stable dimers.

Ribulose-1,5-bisphosphate carboxylase/oxygenase[1] (EC 4.1.1.39, rubisco) catalyzes the carboxylation of ribulose-P_2 by atmospheric CO_2 in all photosynthetic organisms. The enzyme from the photosynthetic bacteria *Rhodospirillum rubrum* is a dimer of identical large chains (L_2), each of relative molecular mass (M_r) 55 000. Intersubunit interactions have structural as well as functional importance, since some of the participant amino acids are active site residues (Schneider et al., 1986). Extensive biochemical and structural data have provided considerable insight into the mechanism of catalysis [for review, see Andrews and Lorimer (1987) and Schneider et al. (1992)]. Site-directed mutagenesis studies defined the requirement of particular amino acid residues in the intersubunit interaction (Smith et al., 1988; Mural et al., 1990). However, because of difficulties in establishing reversible dissociation conditions for the *R. rubrum* rubisco, little is known about the energetics of subunit association. High hydrostatic pressure is a general method to induce the dissociation in oligomeric proteins without affecting directly the tertiary structures of the polypeptide chains (Weber, 1987, 1991). Coupling high hydrostatic pressure with fluorescence methods, we describe here the dissociation equilibria and the conformational properties of the monomers obtained under nondenaturing conditions. We determined for the first time the free energy of subunit association in dimeric rubisco and derived its enthalpic and entropic components; we also reexamined the intersubunit affinity of the single-site mutant K168E,[2] previously described as unable to form a stable dimer. In addition, we characterize the binding of the inhibitor CADP and the carbamylation of Lys 191 as stabilizing factors of the dimer and the dissociated monomers, respectively.

MATERIALS AND METHODS

Protein and Enzyme Assay. Recombinant, dimeric rubisco was purified from *Escherichia coli* expressing a plasmid-encoded gene from *R. rubrum* (Pierce & Reddy, 1986; Pierce & Gutteridge, 1986). Plasmid pFL174, expressing the gene for mutant K168E, was a gift of Drs. F. W. Larimer and F.

† This research was supported by a grant from the National Institutes of Health (GM11223) to G.W.

* To whom correspondence should be addressed.

‡ University of Illinois.

§ Du Pont Company.

[1] Abbreviations: Rubisco, ribulose-1,5-bisphosphate carboxylase/oxygenase; bis-ANS, 8,8′-bis(phenylamino)-5,5′-bi[naphthalene]-1,1′-disulfonate; AEDANS, 5-((2-(acetylamino)ethyl)amino)-1-naphthalenesulfonic acid; CADP, 2-carboxy-D-arabinitol 1,5-diphosphate; HPLC, high-performance liquid chromatography.

[2] The single-letter code for amino acids is used to designate site-directed mutants. The first letter refers to the amino acid present in the wild-type protein. The final letter denotes the residue present at the corresponding position in the mutant.

0006-2960/93/0432-5187$04.00/0

C. Hartman and was grown in *E. coli* (Mural et al., 1990). The concentration of rubisco was calculated by using an absorption coefficient of 6.72×10^4 M^{-1} cm^{-1} (Schloss et al., 1982). Catalytic activity was determined by spectophotometric measurement of NADH oxidation in a coupled enzyme assay with an ATP regenerating system (Lilley & Walker, 1974).

Chemicals. 8,8′-Bis(phenylamino)-5,5′-bi[naphthalene]-1,1′-disulfonate (bis-ANS) and *N*-[2-[(iodoacetyl)amino]-ethyl]-5-naphthylamine-1-sulfonic acid (1,5-I-AEDANS) were purchased from Molecular Probes (Eugene, OR). All other reagents were of analytical grade. Water was distilled and filtered through a Millipore water purification system to 18 MΩ resistance. Unless stated otherwise, the experiments were performed in the standard buffer, 0.05 M Tris-HCl (pH 7.6), 1 mM EDTA, 5 mM DTT, and 10% (v/v) glycerol. Addition of 10% (v/v) glycerol was essential to prevent precipitation of samples upon decompression. This stabilizing action of glycerol on proteins subjected to the effect of high pressure has also been observed with phosphorylase A from rabbit muscle (Ruan & Weber, 1993). Any precipitate was removed by a polycarbonate membrane filter (0.2 μm) purchased from Poretics Co. (Livermore, CA). A prepacked Bio-Sil SEC 250 column (600 × 7.5 mm) from Bio-Rad (Richmond, CA) was used for size-exclusion chromatography. A 5-μm reverse-phase (C_8) column (0.46 × 25 cm) from Vydac was used for separation of fragments after proteolytic digestion.

Labeling Procedure. AEDANS–rubisco was prepared by the reaction of a solution of native dimeric rubisco or K168E in 50 mM phosphate buffer (pH 7.0) and 10% glycerol with a 20-fold molar excess of 1,5-I-AEDANS dissolved in the same buffer. The reaction mixture was left for 1 h at room temperature in the dark, to protect the photosensitive reagent, and the unbound dye was removed by extensive dialysis against buffer (0.05 M Tris-HCl (pH 7.6), 1 mM EDTA, 5 mM DTT, and 10% (v/v) glycerol).

Proteolysis and Analysis of Fragments. AEDANS–rubisco was first carboxymethylated (Crestfield et al., 1963) and then incubated for 24 h at 38 °C with TPCK-treated trypsin (two additions of 1.5 mg/mL). The product of the reaction was chromatographed by reverse-phase HPLC using a 5-μm octyl silica column (0.46 × 25 cm) from Vydac. The fragments were eluted using a linear gradient from water containing 0.05% TFA to a mixture of acetonitrile and water (1:1) containing 0.042% TFA over 60 min. For sequence determination, collected peaks were dried in a centrifugal evaporator, incubated with sequencing grade *Staphylococcus aureus* V8 protease (Sigma) for 16 h at 37 °C, and rechromatographed under the same conditions. The eluted peptides were detected by two successive detectors: (1) absorbance monitored at 215 nm and (2) fluorescence emitted at 480 nm upon excitation at 336 nm.

Fluorescence Measurements. Tryptophan lifetime measurements were performed at the Laboratory for Fluorescence Dynamics, Department of Physics, University of Illinois at Urbana-Champaign, in a multifrequency cross-correlation phase and modulation fluorometer that uses the harmonic content of a high repetition rate, mode-locked Nd:YAG laser to synchronously pump a cavity-dumped rhodamine 6G single-jet dye laser (Coherent Co., Palo Alto, CA). The resultant tuned and frequency-doubled 295-nm light was polarized at 55° (Alcala et al., 1985). Emission was observed through a long wavelength pass filter (UV 320, Hoya) with a cutoff at 320 nm. *p*-Terphenyl in cyclohexane (1 ns) was used as lifetime reference. Fluorescence lifetimes of AEDANS-labeled proteins were measured on a multifrequency phase and modulation instrument similar to that described by Gratton and Limkeman (1983). The high-pressure bomb has been described by Paladini and Weber (1981b). Fluorescence spectra were recorded with a computer-controlled photon-counting spectrofluorometer. Polarization measurements at high pressure were made in L-format with a photon-counting polarization fluorometer, and corrections for the small pressure-induced birefrigency of the quartz windows were performed as described by Paladini and Weber (1981b). Updated software for data acquisition and calculations was from ISS (Champaign, IL).

Analysis of Data. The degree of dissociation as a function of pressure was calculated from the anisotropy data by using the equation

$$\alpha_p = [1 + Q(A_p - A_M)/(A_D - A_p)]^{-1} \quad (1)$$

where A_p is the anisotropy of the fluorescence observed at pressure p, A_D and A_M are the anisotropies of the fluorescence from dimer and monomer, respectively, and Q is the ratio of the relative fluorescence yield at high pressure compared to that at low pressure. Anisotropy values are related to the observed polarization (P) by

$$A = 2/3(1/P - 1/3)^{-1} \quad (2)$$

Dissociation constants at atmospheric pressure (K_0) and standard volume changes on association (ΔV^0) were calculated from the relation

$$K(p) = K_0 \exp(p\Delta V^0/RT) \quad (3)$$

where $K(p)$ is the dissociation constant at pressure p. For a dimer–monomer dissociation process,

$$\ln[\alpha_p^2/(1 - \alpha_p)] = p\Delta V^0/RT + \ln(K_0/4C_0) \quad (4)$$

where α_p is the degree of dissociation at pressure p, and C_0 is the molar concentration of protein expressed as dimer (Paladini & Weber, 1981a). ΔV^0 can also be calculated from the displacement along the pressure axis of the dissociation curve when the total protein concentration is changed from C_1 to C_2 (Weber, 1986; Ruan & Weber, 1986; Silva et al., 1989; Erijman & Weber, 1991). For a dimer,

$$\Delta V^0_c = RT \ln(C_2/C_1)/(p_2 - p_1) \quad (5)$$

Rotational relaxation times, ρ, were calculated from the limiting polarization of AEDANS conjugate, P_0, the polarization at pressure p, A_p, and the lifetime, τ, by using the Perrin equation (Perrin, 1926; Weber, 1952),

$$(1/P - 1/3) = (1/P_0 - 1/3)(3\tau/\rho + 1) \quad (6)$$

RESULTS

Intrinsic Fluorescence Emission. Rubisco from *R. rubrum* is a dimer containing six tryptophan residues per monomer (Nargang et al., 1984). The intrinsic fluorescence emission is, as expected, greatly heterogeneous, and its decay can be fitted with 3 lifetimes of 5.6, 2.9, and 0.4 ns, with relative contributions of 0.54, 0.42, and 0.04, respectively. Phase and modulation data for single-site mutant K168E cannot be adequately fitted with three exponentials and exhibit a 1-ns decrease in their average lifetime, compared to the wild-type enzyme. In the absence of Mg^{2+} and $NaHCO_3$, a red shift and a steep decrease in intensity is observed upon compression of the wild-type dimer above 1.5 kbar (Figure 1). These changes in tryptophan emission with pressure are independent of protein concentration in the range 0.1–4 μM, indicating

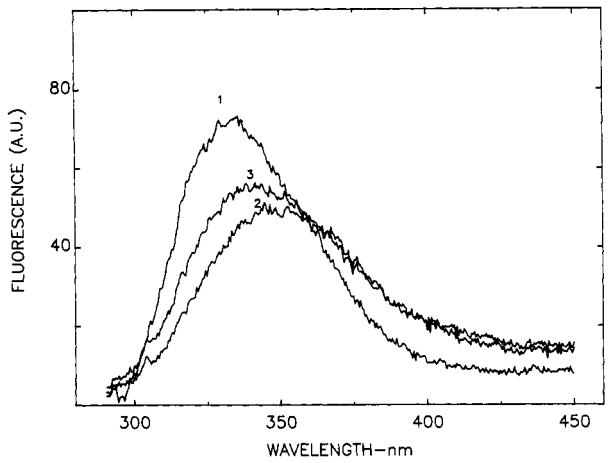

FIGURE 1: Intrinsic fluorescence emission spectra of 200 nM rubisco in 0.05 M Tris-HCl, 1 mM EDTA, 5 mM DTT, and 10% glycerol at pH 7.6 and 2 °C, measured at atmospheric pressure (curve 1), at 2.0 kbar (curve 2), and 30 min after release of pressure (curve 3). Excitation wavelength: 295 nm.

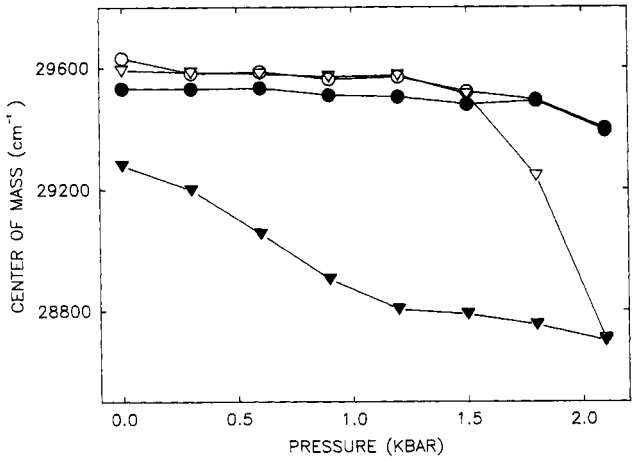

FIGURE 2: Center of spectral mass of the intrinsic fluorescence of wild-type rubisco as a function of applied pressure. Each point is the computed average mass of a spectrum scanned between 300 and 420 nm, upon excitation at 295 nm. The data are for increasing pressures in buffer A containing 2 mM EDTA (▽), decreasing pressures in the same buffer (▼), and increasing pressure in the presence of 100 mM $NaHCO_3$ and 15 mM $MgCl_2$ (○) or these compounds and 1 μM CADP (●). Protein concentrations: 8×10^{-8} M.

Table I: Effect of Temperature and Protein Concentration on Dissociation of Rubisco by Pressure[a]

method[b]	temp (°C)	prot concn ($\times 10^{-7}$ M)	ΔV^0 (mL mol^{-1})	K_{atm} ($\times 10^{-10}$ M)
A	2	4	130	5
A	2	40	122	2
B	2	3.5	118	3
B	2	3	102	3.3
B	8	3	100	2.8
B	15	5	136	1.5
B	15	0.5	166	1.2
B	15	3	106	1.8
A[c]	2	30	133	480
B[c]	2	26	110	740

[a] All experiments were done in buffer containing 0.05 M Tris-HCl, pH 7.6, 10 mM DTT, 15 mM $MgCl_2$, and 100 mM $NaHCO_3$. [b] Methods: (A) Polarization of intrinsic fluorescence. The excitation wavelength was 295 nm; emission was detected through a WG 320 cutoff filter. (B) Polarization of fluorescence of the AEDANS conjugate. The excitation wavelength was 365 nm; emission was observed through a Corning 3-72 cutoff filter and a 2-mm layer of $NaNO_2$, 2 M. [c] Data for K168E.

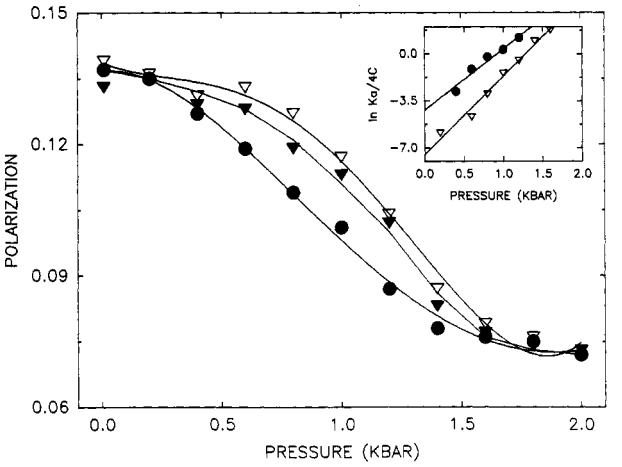

FIGURE 3: Changes in the polarization of the intrinsic fluorescence of rubisco induced by pressure for two protein concentrations at 2 °C. The buffer used was 0.05 M Tris-HCl, 1 mM EDTA, 5 mM DTT, 100 mM $NaHCO_3$, 15 mM $MgCl_2$, and 10% glycerol at pH 7.6. The excitation wavelength was 295 nm; emission was observed through a Corning 0-52 cutoff filter. Shown are data for pressure increase (▽) and decrease (▼) for 4×10^{-6} M rubisco and pressure increase for 4×10^{-7} M rubisco (●). Inset: Plot of ln $K_{diss}/4C_0$ vs pressure for 4×10^{-6} M rubisco (▽) and 4×10^{-7} M rubisco (●).

that dissociation alone cannot be considered the cause of spectral shift. After decompression the changes in emission are only partially reversible, and the activity of the enzymatic solution is greatly diminished. However, no dramatic changes in the fluorescence lifetime are detected: the decay can be fitted with three components of 6.3, 2.4, and 0.2 ns, with fractional intensities of 0.54, 0.42, and 0.04, respectively. On the other hand, when the solution of rubisco subjected to pressurization contains excess of activators and 10% (v/v) glycerol, no appreciable change in the intrinsic emission properties is observed at pressures at which other methods indicate complete dissociation (Figure 2). These results imply that none of the tryptophan residues responsible for the bulk emission are exposed to a polar environment upon dissociation in the carbamylated enzyme. As seen from the crystallographic structure, all six tryptophans are buried in the interior of the protein (Schneider et al., 1990) and are not expected to become exposed to the solvent after dissociation unless a major change in conformation takes place. Nonetheless, local motions of at least some of the tryptophan residues increase as the restrictions at the interface are lessened upon dissociation, and a decrease of the polarization of the intrinsic fluorescence of rubisco as a function of applied pressure was observed in the presence of the activators. In addition, under these conditions the dissociation is fully reversible, according to the recovery of spectroscopic properties and catalytic activity. Figure 3 shows that the decrease in polarization of the intrinsic fluorescence is dependent on protein concentration, as expected if subunit dissociation is the cause of the observed change. The apparent standard volume change on association (ΔV^0) was calculated as described above, and the results are shown in Table I. For a 10-fold change in protein concentration, the difference in pressure necessary to promote 50% dissociation ($\Delta p_{1/2}$) is 220 bar, a good indication that the spectroscopic changes result from a shift in the relative concentration of dimer and monomer as a function of pressure. Figure 3 illustrates also a slight but noticeable hysteresis, revealed by a difference between the compression and decompression curves. This behavior requires a partial loss of affinity between subunits upon dissociation (King & Weber, 1986; Silva et al., 1986; Weber, 1987; Ruan & Weber, 1988,

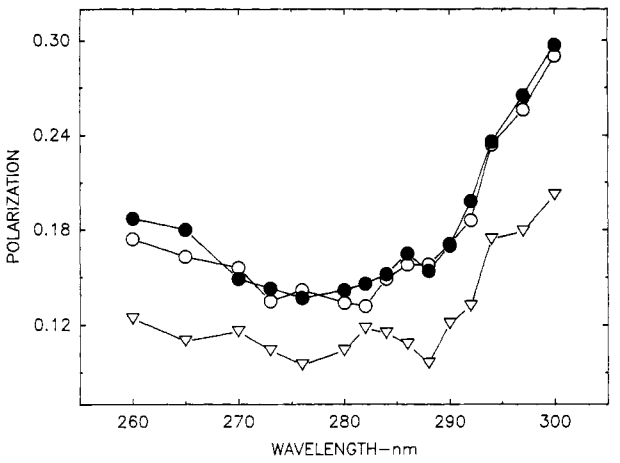

FIGURE 4: Excitation polarization spectra of the Trp fluorescence of 1.6×10^{-6} M rubisco. Emission was detected through a Corning 0-52 filter. Spectra were recorded at atmospheric pressure (●), at 2.0 kbar (▽), and 30 min after release of pressure (○). The buffer was as in Figure 2. All observations were recorded at 2 °C.

1989). The quaternary complex rubisco–Mg^{2+}–CO_2–CADP was not dissociated by pressures up to 2.0 kbar (not shown). As noticed from the excitation polarization spectra (Figure 4), in addition to the increase in mobility, the monomers displayed a blue shift in the secondary maximum of polarization at 290 nm (Valeur & Weber, 1976) which implies a relative blue shift of the L_b transition. This phenomenon was observed before in the drifted glyceraldehyde-3-phosphate dehydrogenase from yeast (Ruan & Weber, 1989) and may be indicative of an increased exposure of the residues involved to a more polar environment. When identical samples were studied at 25 °C, a low polarization plateau was not observed at high pressure, indicating that at this temperature the dissociated monomers might not be completely stable.

Preparation of AEDANS–Rubisco. The labeling stoichiometry was determined from the difference spectrum and the absorbance at 337 nm by using $\epsilon_{337nm} = 6.0 \times 10^{-3}$ M^{-1} cm^{-1}, which is the molar extinction coefficient for the product of the reaction of 1,5-I-AEDANS with *N*-acetylcysteine (Hudson & Weber, 1973), also used for methionyl-tRNA synthetase (Ferguson & Yang, 1986). When the modification of rubisco was carried out as described in the Materials and Methods section, the resulting stoichiometry was 1 mol of AEDANS per mol of monomer, and the enzymatic activity of rubisco was preserved. Cysteine residues are essential for spinach rubisco activity, and although no homology has been found between any of the active site peptides from spinach enzyme and any of the cysteinyl peptides from *R. rubrum* enzyme (Stringer et al., 1981), it was of interest to establish the location of the SH group modified by our procedure. As shown in Figure 5A,B, more than 90% of the fluorescence is carried by a single peptide. We isolated the peptide containing the AEDANS-labeled cysteine. No peak containing modified cysteine appeared in mass spectrometry FAB spectra scanned up to m/z 3500. After a second proteolytic digestion, this time with *S. aureus* V8 enzyme, FABMS showed quasimolecular ions at m/z 959.8 and 997.9 of ($M + H^+$) and ($M + K^+$), respectively, corresponding to the fragment VECTTDD, comprising residues 56–62 of rubisco. This fragment is located in a flexible loop region, disordered in the crystals obtained by Schneider et al. (1990). Cysteine 58 is at the surface of the protein and is the only one, out of the five cysteine residues in each subunit, exposed to the solvent in native rubisco. This selective reactivity of 1,5 I-AEDANS, consistent with the

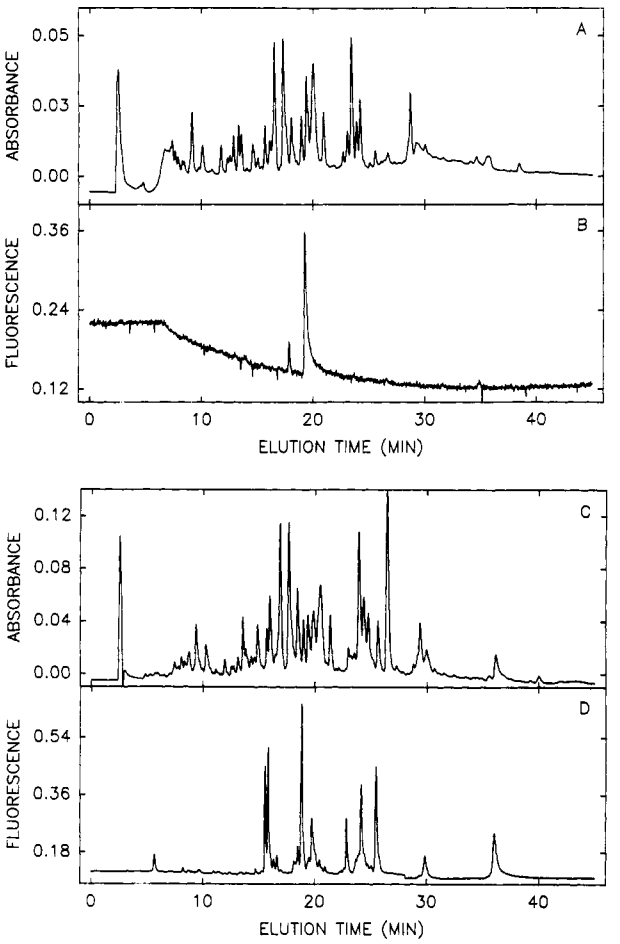

FIGURE 5: Reverse-phase HPLC of tryptic peptides obtained from reduced and S-carboxymethylated AEDANS–rubisco using a 5-μm octyl silica column (0.46 × 25 cm) from Vydac. The fragments were eluted using a linear gradient from water containing 0.05% TFA to a mixture of acetonitrile and water (1:1) containing 0.042% TFA. The labeling reaction was carried out for 1 h at 23 °C and at atmospheric pressure (A,B) or 2.0 kbar (C,D). Detection was by absorbance at 215 nm (A,C) or by fluorescence emission at 480 nm (excitation: 336 nm) (B,D).

crystal data, was thereafter used as a probe for conformational changes upon compression. A parallel reaction was carried out under the conditions described above, except that in this case the reaction was left to proceed at 2.0 kbar. Although no cysteine residue is present in the interface between subunits, after tryptic digestion and reverse-phase chromatography a completely different pattern of the fluorescent eluant was observed (Figure 5C,D). Seven major fluorescent peaks are observed; that is two more peptides than the maximum of five predicted in the case of complete labeling, probably due to incomplete cleavages at trypsin sites.

Dissociation of AEDANS–Rubisco. Direct observation of the dissociation induced by an increase in pressure was also obtained by changes in the polarization of the fluorescence of the AEDANS moiety covalently attached to rubisco. The augmented depolarization observed upon compression reflects the faster overall motion of the monomers compared to the dimers. The lifetime of the fluorescence of the protein conjugate was fitted with two components, 19.0 and 5.1 ns, which accounted for 94% and 6% of the emission, respectively. When an average value of 18.2 ns was employed, the rotational relaxation time derived from the Perrin equation was 137 ns for the dimer and 73 ns for the monomer, in reasonable agreement with their respective sizes. Figure 6 shows that an increase in rubisco concentration from 5×10^{-8} M to 5×10^{-7}

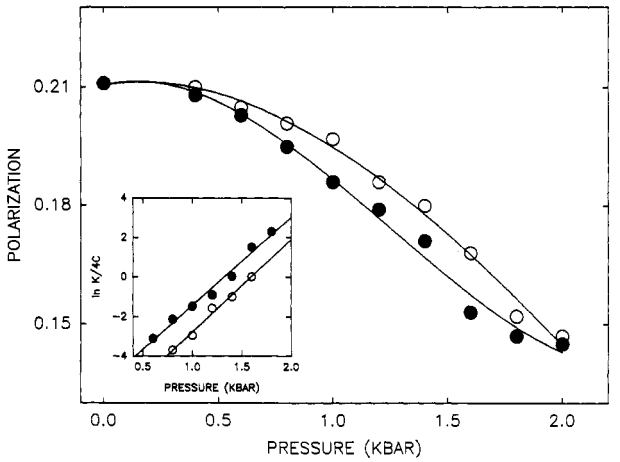

FIGURE 6: Fluorescence polarization changes of AEDANS–rubisco measured at different total protein concentrations. The buffer was as in Figure 2. The excitation wavelength was 335 nm. Emission was detected through a Corning 3-72 filter and a layer of 2 M $NaNO_2$ (2 mm). Protein concentrations were 5×10^{-7} M (○) and 5×10^{-8} M (●) at 2 °C. Inset: Plot of ln $K_{diss}/4C_0$ vs pressure for 5×10^{-7} M protein (○) and 5×10^{-8} M protein (●).

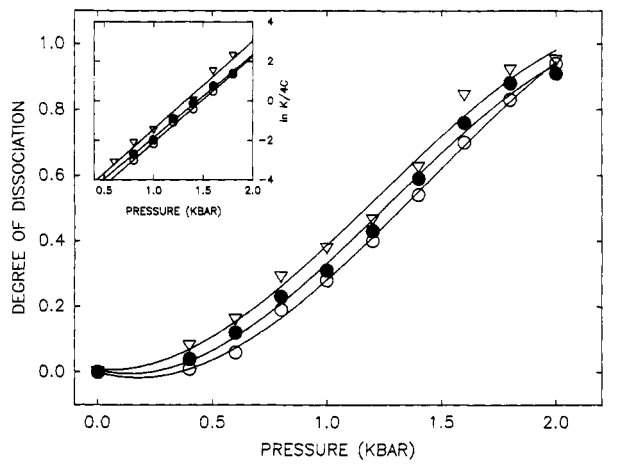

FIGURE 7: Effect of temperature on pressure-induced dissociation of rubisco. Degrees of dissociation were determined by the polarization of the fluorescence of 3.5×10^{-7} M AEDANS–rubisco conjugates, excited at 335 nm. Emission was detected through a Corning 3-72 filter and a 2 M $NaNO_2$ layer (2 mm). Experiments were performed at 2 °C (▽), 8 °C (●), and 15 °C (○). The buffer was as in Figure 2. Inset: Plot of ln $K_{diss}/4C_0$ vs pressure at 2 °C (▽), 8 °C (●), and 15 °C (○).

M shifted the pressure required for half-dissociation by 250 bar; this magnitude, as well as the value of 220 bar obtained from the polarization of the intrinsic fluorescence, is comparable to the theoretical value of 325 bar (Weber, 1986), indicating the stochastic character of the dimer–monomer equilibrium (Erijman & Weber, 1991; Weber, 1991).

Figure 7 shows plots of the pressure–dissociation curves of 3×10^{-7} M solutions of rubisco labeled with AEDANS at 2, 8, and 15 °C. As pointed out previously, the instability of the dissociated species at higher temperatures precluded the analysis over a wider temperature range. A plateau is reached in all the cases at high pressures, indicating completion of the dissociation process. As seen in Table I, which summarizes the results of analysis, the parameters recovered from the polarization of the intrinsic fluorescence and the polarization of the AEDANS-labeled conjugate are in close agreement. The volume changes upon association are in the range of 122 ± 20 mL mol^{-1}. The change in enthalpy of association (ΔH) and the entropic component ($T\Delta S$) were derived from the

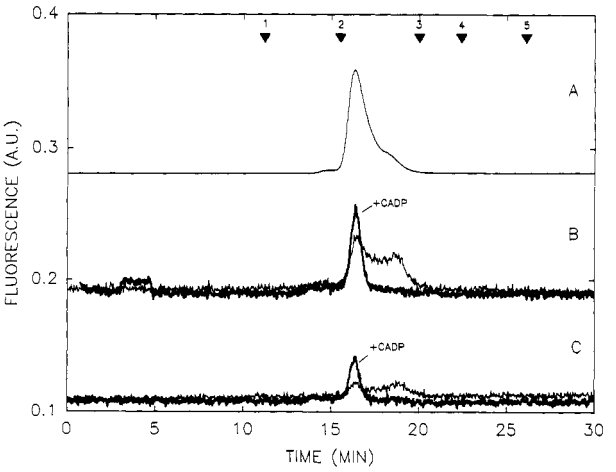

FIGURE 8: Effect of concentration and CADP on dimer–monomer equilibrium in K168E rubisco. Samples were loaded after 1 h of equilibration at room temperature onto a Bio-Sil SEC 250 size-exclusion column. Elution was monitored by using a fluorescence detector (excitation, 280 nm; emission, 335 nm). The amounts of protein loaded were (A) 80 μg, (B) 3.2 μg, and (C) 1.6 μg. The molecular weight standards were (1) thyroglobulin (M_r = 670 000), (2) γ-globulin (M_r = 158 000), (3) ovalbumin (M_r = 44 000), (4) myoglobin (M_r = 17 000), and (5) vitamin B12 (M_r = 1350).

dependence of the dissociation constant on the temperature:

$$\ln K_0 = \Delta H/RT - \Delta S/R \quad (7)$$

At pH 7.6 and atmospheric pressure, the free energies of association of the dimers were determined as −11.8 kcal mol^{-1} at 0 °C, −12.3 kcal mol^{-1} at 8 °C, and −12.9 kcal mol^{-1} at 15 °C. The instability of the monomers at temperatures higher than 20 °C precluded the determination of the thermodynamic parameters over a wide range. The unfavorable enthalpic contribution to the association (6.0 kcal mol^{-1}), which reflects a large enthalpy of hydratation of the subunit interfaces, is compensated by an increase in entropy, $T\Delta S$ (18.9 kcal mol^{-1} at 15 °C). The entropic contribution is thus the driving force responsible for the stability of rubisco as a dimer under standard conditions.

Chromatographic Profile of Mutant K168E. The pattern of gel filtration chromatography of K168E at a concentration of 1 μM is characterized by a single peak having an elution time of 17 min (corresponding to a M_r of 110 000), with a noticeable shoulder at longer times (Figure 8A). By contrast, two resolved peaks are observed at lower concentration (Figure 8B,C); the additional peak elutes 2 min after the first one, the elution time expected for a globular protein of M_r = 55 000 (monomer). Both peaks are well resolved, indicating slow exchange between subunits, compared with the time scale of the chromatographic run. This may appear in contradiction with the observed relaxation time of the dissociation upon compression of 4–5 min, as determined by polarization of the fluorescence (data not shown). However, it has been demonstrated that the increase in dissociation of dimers following application of pressure results from an increase in the rate of dissociation k_-, with little effect on the opposing rate k_+ (Silva et al., 1986; Erijman & Weber, 1991). Thus, considering an increase in k_- of 2 orders of magnitude due to the pressure, we estimate a rate of dissociation of 6 h at atmospheric pressure, justifying the observed chromatographic pattern. As illustrated in Figure 8, when the concentration of loaded protein decreases, the monomer:dimer ratio increases, as expected from the law of mass action. From the total amount of protein loaded and the volume containing both peaks an estimation of the concentration in which the mutant dimer is half

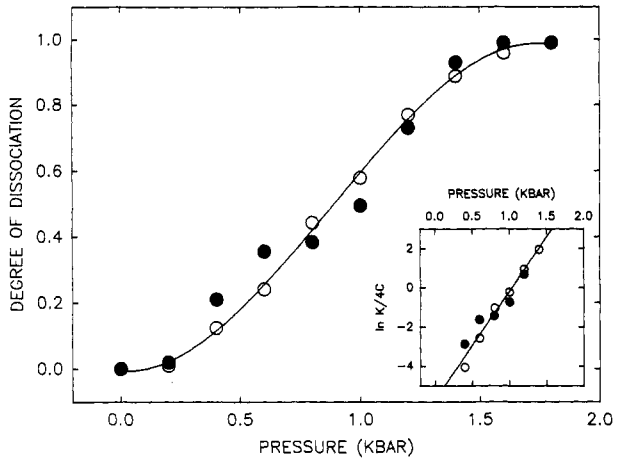

FIGURE 9: Effect of Lys 168 to Glu 168 substitution on intersubunit affinity. Shown are plots of the degree of dissociation vs pressure for a 3 μM solution of K168E, determined by the polarization of the intrinsic fluorescence (●) and by polarization of the AEDANS conjugate fluorescence (○). Experimental conditions were as in Figures 3 and 6, respectively.

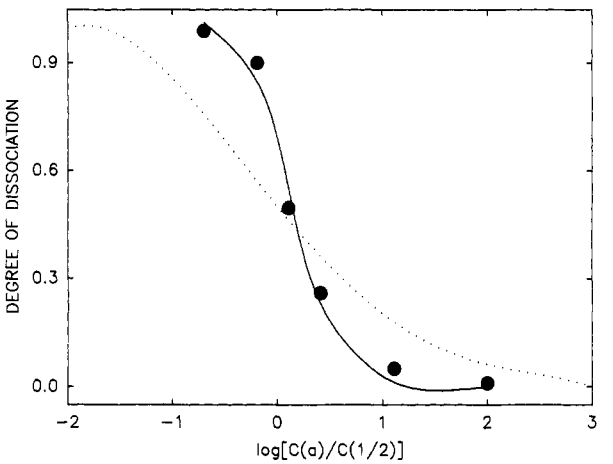

FIGURE 10: Dilution curve calculated from the polarization of the fluorescence of an AEDANS conjugate solution of K168E rubisco at different protein concentrations. The excitation wavelength was 336 nm, and the emission was observed through a Corning 3-72 filter plus a 2-mm layer of $NaNO_2$ (2 M). Background fluorescence was substracted. The dotted line corresponds to the theoretical dilution curve for a dimer–monomer equilibrium with $C_{1/2}$ = 100 nM.

dissociated gives a value of 80 nM. In the presence of the transition-state analog CADP a single peak eluting at 17 min of the quaternary complex is observed even at the lowest concentration (Figure 8C). Since a dimer is required to form the quaternary complex, we confirm with this result not only the stabilizer effect of the inhibitor on the mutant dimer association but also that the mutant K168E can indeed form a stable dimer.

Effect of Lys to Glu Replacement in Position 168 on Intersubunit Affinity. The effect of pressure on the dissociation of K168E was investigated by polarization of tryptophan fluorescence of the mutant and of the AEDANS conjugate of the protein. Conditions and degree of labeling were analogous to those for the wild-type enzyme. Figure 9 shows the excellent agreement between the two spectroscopic methods in the plots of degree of dissociation versus pressure for 3 μM solutions of K168E mutant and a fluorescent conjugate. A logarithmic plot, according to eq 4, gives ΔV = 116 mL mol^{-1}, close to the value obtained for the wild type, and a dissociation constant of 5×10^{-8} M, which is 2 orders of magnitude lower than the wild type. Like for the wild type, a large stabilization results upon formation of the quaternary complex with Mg^{2+}, CO_2, and inhibitor CADP, revealed by a shift of 1.0 kbar of the dissociation curve along the pressure axis toward higher pressures (not shown).

Dilution Curve of Mutant K168E. Given the increased value of the dissociation constant of the mutant enzyme, we attempted to recalculate this parameter by dilution at atmospheric pressure. Polarization of the fluorescence of the AEDANS conjugate was used to determine the degree of dissociation at each concentration. The limiting values of dimer and monomers were found, as expected, to be the same as in the experiments performed at high pressure. The dissociation constant at 2 °C, determined from the midpoint of the dilution curve, was 100 nM (Figure 10), in agreement with the values obtained using high-pressure techniques. An additional feature can be pointed out from these experiments: a decrease in the concentration span was observed, compared with the theoretical value of 2.86 logarithmic units (Figure 10). This effect was previously described in other dimers (Shore & Chakrabarty, 1976; Xu & Weber, 1982; Silva et al., 1992), the result of a concentration-dependent equilibrium constant, due to a conformational drift of separated monomers.

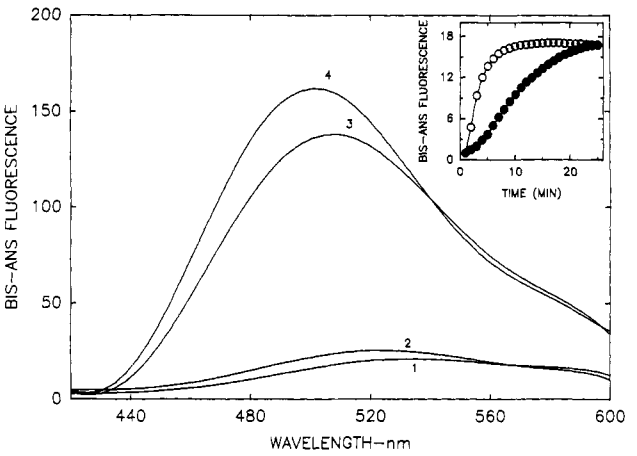

FIGURE 11: Binding of bis-ANS (10^{-6} M) to rubisco (10^{-7} M) at 2 °C and 2.0 kbar (curves 2–4) in 0.05 M Tris-HCl, 5 mM DTT, and 10% glycerol at pH 7.6. The excitation wavelength was 365 nm. Curve 1, control at atmospheric pressure; curve 2, with 100 mM $NaHCO_3$ and 15 mM $MgCl_2$; curve 3, with 100 mM $NaHCO_3$, 15 mM $MgCl_2$, and 2 μM CADP; curve 4, with 2 mM EDTA. Inset: Time course of the fluorescence intensity changes upon compression to 2.0 kbar of bis-ANS–rubisco in the presence of 2 mM EDTA (○) or 100 mM $NaHCO_3$ and 15 mM $MgCl_2$ (●).

Binding of Bis-ANS to Rubisco. Bis-ANS undergoes changes in its fluorescence properties as a result of noncovalent interactions with hydrophobic surfaces of proteins, especially in the neighborhood of positive charges (Rosen & Weber, 1975). As seen in Figure 11, there is a 17-fold increase in the yield of fluorescence of the free ligand and a spectral blue shift of 35 nm when bis-ANS is subjected to high pressure in the presence of rubisco, compared to the same solution before compression. No changes in the spectral properties of bis-ANS fluorescence were observed upon compression of a solution of free fluorophore or one containing fluorophore with the quaternary complex of rubisco, Mg^{2+}, CO_2, and CADP. The kinetics of binding is different depending on the state of activation of the enzyme: for the nonactivated rubisco the half-time of binding of the ligand (5–6 min) is coincident with the half-time for subunit dissociation (determined through the decrease of polarization of the AEDANS conjugate). Carbamylated rubisco, on the other hand, binds bis-ANS to the same extent as the inactive protein but in a slower fashion

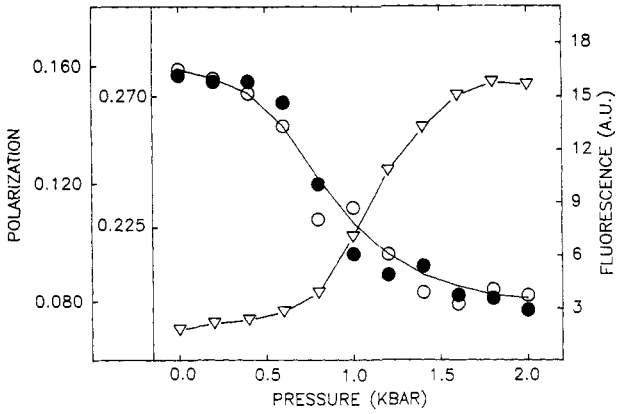

FIGURE 12: Effect of pressure upon binding of bis-ANS to rubisco. Shown are plots of bis-ANS fluorescence intensity (▽) and fluorescence polarization on excitation at 365 nm (●) and polarization of bis-ANS fluorescence on excitation at 435 nm (○). All observations were recorded at 2 °C in 0.05 M Tris-HCl, 2 mM EDTA, 5 mM DTT, and 10% glycerol at pH 7.6.

(inset of Figure 11). One explanation consistent with these results is that the extensive binding of the bis-ANS arises from the exposed surfaces of the monomer upon dissociation and probably by a conformational change of the isolated monomer. The lag observed in the activated enzyme is due to decarbamylation of Lys 191 of the monomer, followed by binding of bis-ANS to a cationic protein surface close to the active site, with subsequent stabilization of a conformationally drifted monomer. The stabilizer effect of bis-ANS is confirmed by incubation at atmospheric pressure of the chromophore with a 1 μM solution of the mutant K168E. A very slow increase in fluorescence with displacement to the maximum of 480 nm (half-time = 4 h) reveals a shift in the dimer–monomer equilibrium of the mutant toward the dissociated form (not shown). Attempts to isolate this complex failed due to its great tendency to be adsorbed by most separation matrices. As pressure is raised, the polarization of the fluorescence of bis-ANS decreases in parallel with increasing intensities (Figure 12). Excitation at the red edge of the absorption band rendered the same result, indicating that the depolarization is not due to energy transfer between identical molecules bound to the protein (Figure 12). With a limiting polarization of 0.299 (derived from a Perrin plot) and an observed average lifetime of 6.8 ns (with a main component of 7.1 ns, responsible for 85% of the emission, and a second of 0.9 ns, responsible for 15% of the emission), the calculated rotational relaxation time was 17.1 ns, suggesting a considerable local mobility of the bound probe.

DISCUSSION

This paper provides some quantitative aspects of the thermodynamic properties of dimeric rubisco from *R. rubrum* as well as a characterization of the stability of the dissociated monomers. High hydrostatic pressures allow the determination of dissociation using concentrations that are nearly 3 orders of magnitude larger than the dissociation constant. The dimer and the dissociated subunits are each characterized by a distinctive value of the fluorescence polarization, whether the change is due to the decrease in volume of the particles (Figure 6) or to the increase in local rotations of the aromatic probe (Figures 3 and 4). Thus, we were able to determine the free energies of association of the monomers at atmospheric pressure. Comparison with other oligomeric systems, particularly dimers and tetramers, reveals a striking similarity both in the free energies of association, usually found in the range of −11 to −14 kcal^{-1}, and in the change in volume on association, a quantity that ranges between 100 and 200 mL mol^{-1}. The large and positive entropic contribution ($T\Delta S$) of 18.9 kcal mol^{-1} (at 15 °C) indicates that the monomer association is entropy driven, providing one more example of what has been found in essentially all cases so far studied, with the enthalpy changes opposing the formation of the dimer from the isolated protomers. A discussion of the origin of this large excess of entropy will appear elsewhere (Weber, 1993).

The agreement between ΔV calculated by the change in dissociation with increasing pressures and by the change in pressure of half-dissociation when the concentration is decreased 1 order of magnitude approaches that expected for a typical stochastic equilibrium, contrary to the situation observed in tetramers or more complex multisubunit complexes for which the equilibria resemble those of macroscopic systems (Silva & Weber, 1988; Silva et al., 1989; Ruan & Weber, 1988, 1989; Erijman & Weber, 1991).

2-Carboxy-D-arabinitol 1,5-diphosphate (CADP) is a carboxylation reaction transition-state analog that inhibits rubisco by binding to the activated enzyme to form an extraordinary stable quaternary complex E–CO_2–Me–CADP with a 1:1:1:1 stoichiometry (Miziorko, 1979; Pierce et al., 1980). Crystallographic analysis has revealed that binding of the transition-state analog to the nonactivated enzyme is different from the binding of the analog to activated spinach rubisco (Lundqvist & Schneider, 1989). At the higher pressure reached in this study no sign of dissociation of the quaternary complex for the wild-type enzyme was detected by any of the methods of analysis used. The large stabilization against pressure-induced subunit dissociation of the quaternary complex is due to a strong negative free energy coupling between inhibitor binding and subunit interaction. No stabilization was observed when CADP was bound to the nonactivated enzyme, which emphasizes the specificity of the coupling between ligand binding and subunit–subunit interaction in the stabilization of the complex. The mutant K168E is also able to participate in a quaternary complex with the transition-state analog. However, since the initial stability of the mutant dimer is lowered by the single amino acid replacement, it is possible to estimate the magnitude of stabilization by binding of the inhibitor. From the expression $\Delta G_s = -\Delta p_{1/2}\,\Delta V^0$, with a volume change on association of 120 mL mol^{-1}, a shift of 1 kbar in the pressure required to promote half-dissociation results in a free energy of stabilization of −2.3 kcal mol^{-1}.

Recently, Lu et al. (1992) performed an evaluation of the electrostatic potential at the active site of rubisco. Comparing the electrostatic contribution to the binding energy of the subunits, for the wild-type protein and the mutant K168E, they calculated an energy of destabilization for the latter of 9 kT, with an estimated error of 10% (Lu et al., 1992). The value of 4.9 kcal mol^{-1} at 2 °C is to be compared with approximately 2.8 kcal mol^{-1} for the *overall* difference in free energy of association, obtained from fluorescence polarization, dilution experiments, and size-exclusion chromatography. We find these two figures to be in reasonable agreement, and since for the wild-type protein $\Delta H > 0$, it is evident that the destabilization in the mutant must imply an even larger positive value for the enthalpy of association. We also note that from this value it is clear that K168E must have a negative ΔG of association (that is, it exists as a dimer) in the range of biologically relevant temperatures. The ability of the mutant protein to form a quaternary complex with the transition-

state analog CADP in the presence of Mg^{2+} and CO_2 leaves no doubt as to its state of association.

Another point of interest is the contribution of carbamylation to the stability of the isolated monomers of *R. rubrum* rubisco. The molecular mechanism for the activation of rubisco for both carboxylation and oxygenation involves derivatization of the ϵ-amino of a specific lysine residue (Lys 191 in *R. rubrum*) by CO_2 to form a labile carbamate, which is further stabilized by binding of a magnesium ion (Lorimer, 1981). Small angle neutron scattering experiments did not reveal structural differences in solution between activated and deactivated rubisco (Donnely et al., 1984). The crystal structure of the ternary complex between rubisco, Mg^{2+}, and activator CO_2 also showed absence of any major conformational change, compared to the nonactivated enzyme (Lundqvist & Schneider, 1991). Mg^{2+} has been invoked to be essential for proper orientation of the substrate (Lundqvist & Schneider, 1989) and polarization of the bond between carbon C2 and oxygen (Andrews & Lorimer, 1987). Upon carbamylation the positive charge of the ϵ-amine group of Lys 191 is replaced by the negatively charged carbamate. Mg^{2+} is coordinated to residues Asp 193 and Glu 194 of one subunit and to the carbamate. The side chain of the conserved Asn 111 of the other subunit is also close to the Mg^{2+}, but as discussed by Lindqvist & Schneider (1991), from the observed differences in the metal-binding site between subunits the Asn side chain does not seem to be important for the formation of the ternary complex. When the dimer is forced to dissociate, additional sites become available for the binding of bis-ANS, every cysteine reacts against the 1,5-I-AEDANS, and changes in the fluorescence emission of internal tryptophan residues reveal an increased exposure to the solvent. It is likely that when the subunits become separated, an intramolecular interaction between the ϵ-amino group of Lys 191 and some acidic group produces a conformational change that eventually results in the unfolding and aggregation of the dissociated protomers. It is a remarkable and unexpected observation that specific formation of carbamate at that position in the wild-type enzyme stabilized by coordination of Mg^{2+} with the side chains prevents that *conformational drift* from happening. Time-dependent changes in subunit affinity and spectroscopic properties and loss of enzyme activity on decompression have been previously observed in other oligomeric proteins following subunit dissociation, regardless of the cause of separation. The name used to refer to this phenomenon indicates a time-dependent process that cannot be easily described as a chemical equilibrium between well-defined forms. In the case of dimeric rubisco, the concentration-independent and irreversible process that occurs at pressures higher than 1.5 kbar, revealed by a decrease in the tryptophan quantum yield and progressive binding of bis-ANS, is a further indication of a drift in conformation of the dissociated monomers. The same conclusion applies to the decreased concentration span observed in dilution experiments with mutant K168E (Xu & Weber, 1982; Weber, 1986). For this phenomenon to be observed, it is necessary that the conformational drift be rapidly reversed on association, a quality that the pressure experiments show is lacking in the wild type. For the nonactivated enzyme the recovery of the original properties of the enzyme becomes progressively less complete as the pressure is raised and the incubation time is lengthened, because the loss of contacts between subunits provokes a significant unfolding of the dissociated protomers that aggregate nonspecifically upon decompression. Some of the properties of the species obtained upon dissociation, namely, the red-shifted tryptophan emission relative to that of the native dimer, binding of hydrophobic probes, and instability at high concentrations and at temperatures above 15 °C, resemble those of the folding intermediate found by Lorimer and co-workers (Viitanen et al., 1990; van der Vies et al., 1992) in reconstitution experiments after chemically induced denaturation of rubisco. Unfortunately chaperonin cpn60 is an oligomeric complex, also dissociated by high pressure (not shown); therefore its affinity for the rubisco monomers at high pressure could not be tested. Activation by CO_2 and metal ions with formation of a ternary complex is a property common to all rubiscos regardless of their taxonomic origin (Lorimer & Maziorko, 1983; Andrews & Lorimer, 1987). Interestingly, addition of Mg^{2+} and CO_2 enhances the thermal stability of the hexadecameric rubisco without any effect on the subunit cooperativity (Tomimatsu & Donovan, 1981). It was also recently found that pretreatment of the enzyme with Mg^{2+} and CO_2 prevents the inactivation that is known to occur in spinach rubisco upon storage of dilute solutions in the cold (Heuer & Portis, 1990). As demonstrated by King and Weber (1986), by hybridization of the isozymes of lactate dehydrogenase at low temperature, and later confirmed using energy transfer between differentially labeled subunits of glyceraldehyde-3-phosphate dehydrogenase (Erijman & Weber, 1993), the mechanism of cold inactivation involves a process of dissociation, conformational drift of the separated subunits, and reassociation into drifted, inactive oligomers, exactly as it happens with pressure-induced dissociation. The similarity of the effects of CO_2 and Mg^{2+} further supports the suggested structural role for carbamylation in the stability of subunits in ribulose-bisphosphate carboxylases. The stabilization effect of the monomer by means of carbamate formation, opposing a fast turnover of the protein in the living cells, could give a possible answer to the still puzzling question of why rubisco is not permanently activated.

ACKNOWLEDGMENT

We thank Dr. F. C. Hartman and Dr. F. W. Larimer (Oak Ridge National Laboratory) for making available to us the plasmid encoding the mutant rubisco K168E, Ms. Kasia Janota for performing the mass spectroscopy, and Mr. Rong Huang for advice on sequence determination of the proteolytic fragments.

REFERENCES

Alcala, R., Gratton, E., & Jameson, D. M. (1985) *Anal. Instrum. 14*, 225–250.

Andrews, T. J., & Lorimer, G. H. (1981) in *The Biochemistry of Plants* (Hatch, M. D., Ed.) Vol. 10, pp 131–218, Academic Press, Orlando, FL.

Crestfield, A. M., Moore, S., & Stein, W. M. (1963) *J. Biol. Chem. 238*, 622–627.

Donnelly, M. I., Hartman, F. C., & Ramakrishan, V. (1984) *J. Biol. Chem. 259*, 406–411.

Erijman, L., & Weber, G. (1991) *Biochemistry 30*, 1595–1599.

Erijman, L., & Weber, G. (1993) *Photochem. Photobiol. 57*, 411–415.

Ferguson, B. Q., & Yang, D. C. H. (1986) *Biochemistry 25*, 2743–2748.

Goloubinoff, P., Christeller, J. T., Gatenby, A. A., & Lorimer, G. H. (1989) *Nature 342*, 884–889.

Gratton, E., & Limkeman, M. (1981) *Biophys. J. 44*, 315–323.

Heuer, B., & Portis, A. R., JR. (1990) *Plant Physiol. 93*, 1511–1513.

Hudson, E. N., & Weber, G. (1973) *Biochemistry 12*, 4154–4161.

King, L., & Weber, G. (1986) *Biochemistry 25*, 3632–3637.

Lilley, R. McC., & Walker, D. A. (1974) *Biochim. Biophys. Acta 358*, 226–229.
Lorimer, G. H., & Miziorko, H. M. (1980) *Biochemistry 19*, 5321–5328.
Lorimer, G. H. (1981) *Biochemistry 20*, 1236–1240.
Lundqvist, T., & Schneider, G. (1989) *J. Biol. Chem. 264*, 7078–7083.
Lundqvist, T., & Schneider, G. (1991) *Biochemistry 30*, 904–908.
Miziorko, H. M. (1979) *J. Biol. Chem. 254*, 254–258.
Miziorko, H. M., & Lorimer, G. H. (1983) *Annu. Rev. Biochem. 20*, 507–535.
Mural, R. J., Soper, T. S., Larimer, F. W., & Hartman, F. (1990) *J. Biol. Chem. 265*, 6501–6505.
Nargang, F., McIntosh, L., & Sommerville, C. (1984) *MGG, Mol. Gen. Genet. 193*, 220–224.
Paladini, A. A., & Weber, G. (1981a) *Biochemistry 20*, 2587–2593.
Paladini, A. A., & Weber, G. (1981b) *Rev. Sci. Instrum. 52*, 419–427.
Perrin, F. (1926) *J. Phys. Radium 7*, 390–401.
Pierce, J., & Gutteridge, S. (1986) *Appl. Environ. Microbiol. 49*, 1094–1100.
Pierce, J., & Reddy, G. S. (1986) *Arch. Biochem. Biophys. 245*, 483–493.
Pierce, J., & Tolbert, N. E., & Barker, R. (1980) *Biochemistry 19*, 934–942.
Rosen, C.-G., & Weber, G. (1969) *Biochemistry 8*, 3915–3920.
Ruan, K. C., & Weber, G. (1988) *Biochemistry 27*, 3295–3301.
Ruan, K. C., & Weber, G. (1989) *Biochemistry 28*, 2144–2153.
Ruan, K. C., & Weber, G. (1993) *Biochemistry* (in press).
Schloss, J. V., Phares, E. F., Long, M. V., Norton, I. L., Stringer, C. D., & Hartman, F. C. (1982) *Methods Enzymol. 90*, 522–528.
Schneider, G., Lindqvist, Y., Branden, C.-I., & Lorimer, G. H. (1986) *EMBO J. 5*, 3409–3415.
Schneider, G., Anlerson, I., Brānden, C.-I., Knight, S., Lindqvist, Y. A., & Lundqvist, T. (1990) in *Enzymatic and Model Carboxylation and Reduction Reactions for Carbon Dioxide Utilization* (Aresta, M., & Schloss, J. V., Eds.) pp 367–376, Kluwer Academic Publishers, Dordrecht.
Schneider, G., Lindqvist, Y., & Lundqvist, T. (1990) *J. Mol. Biol. 211*, 989–1008.
Shore, J. D., & Chakrabarty, S. K. (1976) *Biochemistry 15*, 875–879.
Silva, J. L., Miles, E. W., & Weber, G. (1986) *Biochemistry 25*, 5780–5786.
Silva, J. L. , Villas-Boas, M., Bonafe, C. F. S., & Meirelles, N. C. (1989) *J. Biol. Chem. 264*, 15863–15868.
Silva, J. L., Silveira, C. F., Correia, A., Jr., & Pontes, L. (1992) *J. Mol. Biol. 223*.
Smith, H. B., Larimer, F. W., & Hartman, F. C. (1988) *Biochem. Biophys. Res. Commun. 152*, 579–581.
Stringer, C. D., & Hartman, F. C. (1986) *Methods Enzymol. 90*, 522–528.
Stringer, C. D., Norton, I. L., & Hartman, F. C. (1981) *Arch. Biochem. Biophys. 208*, 495–501.
Tomimatsu, Y., & Donovan, J. W. (1981) *Plant Physiol. 68*, 808–813.
Valeur, B., & Weber, G. (1976) *Photochem. Photobiol. 25*, 441–444.
van der Vies, S. M., Viitanen, P. V., Gatenby, A. A., Lorimer, G. H., & Jaenicke, R. (1992) *Biochemistry 31*, 3635–3644.
Viitanen, P. V., Lubben, T. H., Reed, J., Goloubinoff, P., O'Keefe, D. P., & Lorimer, G. H. (1990) *Biochemistry 29*, 5665–5671.
Weber, G. (1952) *Biochem. J. 51*, 145–151.
Weber, G. (1986) *Biochemistry 25*, 3626–3631.
Weber, G. (1987) in *High Pressure Chemistry and Biochemistry* (Van Eldik, R., & Jonas, J., Eds.) pp 401–420, D. Riedel, Dordrecht.
Weber, G. (1991) in *New Trends in Biological Chemistry* (Ozawa, T., Ed.) pp 235–238, Japan Scientific Societies Press, Tokyo/ Springer-Verlag, Berlin.
Weber, G. (1993) Relations of bond energy and entropy with volume, pressure and temperature in protein aggregates, in *High Pressure Chemistry, Biochemistry and Material Science* (Winter, R., & Jonas, J., Eds.) NATO Advanced Science Institutes Series C401, Kluwer, Dordrecht.